



## Biosorption of phenol and *o*-chlorophenol from aqueous solutions on to chitosan–calcium alginate blended beads

Siva Kumar Nadavala<sup>a</sup>, Kalyani Swayampakula<sup>a</sup>, Veere M. Boddu<sup>b</sup>, Krishnaiah Abburi<sup>a,\*</sup>

<sup>a</sup> Biopolymers and Thermophysical Laboratories, Department of Chemistry, Sri Venkateswara University, Tirupati 517502, India

<sup>b</sup> Engineer Research & Development Centre-CERL, Champaign, IL 61826, USA

### ARTICLE INFO

#### Article history:

Received 10 June 2007

Received in revised form 13 April 2008

Accepted 16 May 2008

Available online 21 May 2008

#### Keywords:

Biosorption

Chitosan–alginate blended beads

*o*-Chlorophenol

Phenol

### ABSTRACT

Beads of chitosan–sodium alginate are prepared from naturally occurring biopolymers, chitosan (a cationic polysaccharide) and sodium alginate (an anionic polysaccharide). These beads are treated with CaCl<sub>2</sub> in order to improve the stability as well as the sorption capacity of the biosorbent. The resulting chitosan–alginate beads are characterized by BET surface area analysis, Fourier transformer infrared spectroscopy (FTIR) and wide-angle X-ray diffraction (WXR) techniques. The efficiency of the biosorbent is studied by measuring the uptake using the equilibrium batch technique and breakthrough curves obtained from column flow experiments. The effect of pH, contact time, initial concentration of adsorbate and amount of biosorbent on adsorption capacity of the biosorbent is investigated. The equilibrium adsorption data are fitted to first-order and second-order kinetic equations, and to Weber–Morris model. The Freundlich, Langmuir and Dubinin–Radushkevich (D–R) adsorption isotherm models are used for the description of the biosorption process. Further, column break-through curves are obtained and the sorbent loaded with phenol and *o*-chlorophenol is regenerated using 0.1 M NaOH solution. The experimental results suggest that the chitosan–calcium alginate blended biosorbent is effective for the removal of phenol and *o*-chlorophenol from an aqueous medium.

© 2008 Elsevier B.V. All rights reserved.

### 1. Introduction

Phenol and substituted phenols are priority pollutants because of their high toxicity to human beings at low concentrations [1]. Chlorophenols are used extensively in the manufacture of fungicides, herbicides, insecticides, pharmaceuticals, preservatives, glue, paint, fibers, leather, and as intermediates in chemical synthesis [2]. Most of these compounds are recognized as toxic carcinogens. Industrial sources of contaminants such as oil refineries, coal gasification sites, petrochemical units, etc., generate large quantities of phenols. In addition, phenolic derivatives are widely used as intermediates in the synthesis of plastics, colors, pesticides, insecticides, etc. [3]. Degradation of these substances results in the generation of phenol and its derivatives in the environment.

In order to keep waters free from phenolic compounds, different purification methods such as microbial degradation, adsorption, chemical oxidation, incineration, solvent extraction, reverse osmosis and irradiation, are used for removing phenols from wastewater [4]. Adsorption onto activated carbon [5] is commonly used to remove phenolic compounds from wastewater. The high costs of

activated carbon and disposal of spent carbon led to the investigation of alternate cheaper materials such as bentonite [6], rubber seed coat [7], acid-activated bituminous shale [8], zirconium(IV) arsenate–vanadate ion-exchanger [9], rice husk [10], XAD-4 resin [11], and water-insoluble cationic starch and chitosan [12]. Recently several industrial waste materials such as blast furnace sludge, dust, and slag [13], surfactant-modified natural zeolite [14] and activated carbon fibers [15] are used for the removal of phenol and substituted phenols from water.

In recent years, polymeric adsorbents have been used increasingly as an alternative to activated carbon due to their economic feasibility, adsorption–regeneration properties and mechanical strength. Chitosan, a poly(D-glucosamine), is obtained from chitin by deacetylating its acetamide groups with a strong alkaline solution. Chitin is a natural polymer extracted from crustacean shells, such as prawns, crabs, insects, shrimps and fungal biomass. Chitosan has already been described as a suitable natural polymer for the collection of phenolic compounds, through chelation, due to the presence of an amino and hydroxyl groups on the glucosamine unit [16–18]. In most of the studies chitosan has been used in the form of flakes, powder or hydrogel beads.

Sodium alginate, a polysaccharide extracted from seaweed, performed excellently in the removal of organic compounds from water. The soybean peroxidase enzymes were entrapped within

\* Corresponding author. Tel.: +91 9393621986; fax: +91 877 2248499.  
E-mail address: [abburikrishnaiah@gmail.com](mailto:abburikrishnaiah@gmail.com) (K. Abburi).

silica sol-gel/alginate hybrid particles and were used for the removal of phenol [19]. The fungus *Phanerochaete chrysosporium* was immobilized in several polymer matrices such as Ca-alginate, Ca-alginate-polyvinyl alcohol, and pectin, and was then used as a biosorbent for removing 2,4-dichlorophenol (2,4-DCP) in wastewater [20]. Calcium alginate-activated carbon composites were used for phenol adsorption from aqueous solutions [21]. Enzymatic removal of various phenol compounds from synthetic water sample was studied by the use of mushroom tyrosinase and chitosan beads as a function of pH, temperature, tyrosinase dose, and hydrogen peroxide-to-substrate ratio [22]. The adsorption of 4-nonylphenol ethoxylates (NPEs) onto chitosan beads having cyclodextrin was investigated by Aoki et al. [23]. Adsorption of phenol on to chitosan-coated bentonite was also studied by Cheng et al. [24]. Though several studies exist on use of alginates and chitosan separately, we believe that this is the first report on the combined use of chitosan and alginate for the removal of phenolic compounds from water.

The main objective of the present study is to evaluate the use of calcium chloride treated chitosan-sodium alginate beads for removal of phenol and *o*-chlorophenol from aqueous solutions under equilibrium and column flow conditions. Further, the biosorbent is characterized using BET, Fourier transformer infrared spectroscopy (FTIR) and wide-angle X-ray diffraction (WXR) techniques. In addition, the effect of pH, contact time, initial concentrations of adsorbate and adsorbent dose on the extent of adsorption is investigated. Equilibrium adsorption data are fitted to Langmuir, Freundlich and Dubinin-Radushkevich (D-R) isotherms. Further, the adsorbent loaded with phenol and *o*-chlorophenol is regenerated by solution elution method using 0.1 M NaOH as eluent.

## 2. Materials and methods

### 2.1. Materials

Chitosan, with an average molecular weight of 300,000, is purchased from Aldrich Chemical Corporation, USA. Sodium alginate used for blending with chitosan is obtained from Loba Chemie, Mumbai, India, with an average molecular weight of 500,000. Phenol (Ranbaxy, India, A.R. grade) and *o*-chlorophenol (Spectrochem, India, A.R. grade) are used without further purification. Stock solutions are prepared by dissolving 1.0 g of phenol and 1.0 g of *o*-chlorophenol individually in 1 l of double-distilled water. These stock solutions are used to prepare 50, 100, 200, and 300 ppm solutions of phenol and *o*-chlorophenol. The pH of the solutions is adjusted to the required value with 0.01 M HCl and 0.01 M NaOH solutions.

### 2.2. Methods

#### 2.2.1. Preparation of chitosan-calcium (CS/Ca) alginate blended beads

Chitosan (1.5 wt.%) gel is prepared by using 5% acetic acid, and 1.5 wt.% of sodium alginate gel is prepared using double-distilled water. The chitosan and sodium alginate gels are physically mixed in the ratio of 4:1, respectively, in order to obtain chitosan-sodium alginate (CS/SA) gel. This blended solution is stirred for a period of 1 h for homogeneity and kept aside for 1 h to obtain a bubble free solution. Spherical-shaped beads are then prepared by drop-wise addition of CS/SA blended gel into a 10% NaOH precipitation bath. The purpose of adding acidic CS/SA mixture to NaOH solution is to assist rapid neutralization of acetic acid. These spherical-shaped beads are taken from the NaOH bath, and washed several times

with deionized water to a neutral pH. The beads are dried in a freeze drier, followed by oven drying at 60 °C.

The CS/SA blended beads are chemically modified by means of pretreatment with 10% CaCl<sub>2</sub> solution for 24 h at room temperature at a constant pH (5.0). The resulting chitosan-alginate biosorbent beads (CS/Ca) are filtered and washed with deionized water to remove excess calcium, and dried in the oven at 60 °C for 24 h. The pretreated biosorbent is kept in desiccators at room temperature for later use.

Alginate polymer contains D-mannuronic acid and L-guluronic acid. D-Mannuronic acid exists in 1C conformation and is connected in the β-configuration through the 1- and 4-positions and L-guluronic acid has the 1C conformation and is α-1,4-linked in the polymer [25]. Because of the particular shapes of the monomers and their modes of linkage in the polymer, the geometries of the G-block regions, M-block regions, and alternating regions are substantially different. Specifically, the G-blocks are buckled while the M-blocks have a shape referred to as an extended ribbon. If two G-block regions are aligned side by side, a diamond-shaped hole results. This hole has dimensions that are ideal for the cooperative binding of calcium ions. When calcium ions are added to a sodium alginate solution, such an alignment of the G-blocks occurs; the calcium ions are bound between the two chains like eggs in an egg box [26]. Roger et al. [27] reported the complete conversion of sodium alginate in to calcium alginate in about 10 min after addition of sodium alginate to calcium chloride solution.

#### 2.2.2. Batch studies

A series of batch experiments are conducted to explore the effect of influencing factors, such as solution pH, contact time, quantity of adsorbent and the initial concentration of adsorbate. pH of the adsorbate solution is adjusted to set value with 0.01 M HCl and 0.01 M NaOH at the start of the experiment. Batch adsorption experiments are performed by agitating using a mechanical shaker at 150 rpm in 125 ml stopper bottles with specified amount (0.1 g) of adsorbent in contact with 100 ml of phenol or *o*-chlorophenol solution of desired concentration at varying pH for 4 h at room temperature. It is confirmed through the preliminary experiments that the 4 h is sufficient to attain equilibrium between adsorbent and adsorbate. The samples are filtered through Whatman No. 5 filter paper to eliminate any fine particles. Then the concentration of phenol or *o*-chlorophenol solutions is determined by measuring absorbance using Shimadzu UV-240 Spectrophotometer at 268 and 274 nm for phenol and *o*-chlorophenol, respectively. The sorption capacity of the biosorbent is determined by material balance of the initial and equilibrium concentrations of the solution. Adsorption on the glassware is found to be negligible and is determined by running blank experiments. Each experiment is repeated at least three times and mean values are taken. The amount adsorbed per unit mass of adsorbent at equilibrium is given as follows:

$$Q_e = \left( \frac{C_o - C_e}{m} \right) v \quad (1)$$

where  $Q_e$  (mg g<sup>-1</sup>) is the adsorption capacity at equilibrium,  $C_o$  and  $C_e$  denote the initial and equilibrium concentrations of phenolic solutions (mg l<sup>-1</sup>),  $v$  is the volume of the solution in liters and  $m$  is the mass of the adsorbent used in grams.

#### 2.2.3. Column adsorption studies

Column flow studies are carried out in a column made of Pyrex glass of 1.2 cm i.d. and 15 cm length. The column is filled with CS/Ca alginate beads by tapping so that the column is filled without gaps. The influent solution of known concentration of aqueous solution of phenolic compounds is allowed to pass through the bed at a constant flow rate, 1 ml min<sup>-1</sup>, in down flow manner. The complete

cycle of operation of each column experiment includes three steps: pH precondition of the adsorbate solution, solution flow, and adsorption of solute until column exhaustion occurs. The effluent solution is collected as a function of time and concentrations of phenolic solutions are determined by measuring absorbance using Shimadzu UV-240 Spectrophotometer. All experiments are carried out at room temperature. Breakthrough curves are obtained by plotting volume of the solution passed through the column vs. ratio of the column outlet concentration to the initial concentration,  $C_{\text{outlet}}/C_{\text{inlet}}$ .

#### 2.2.4. Desorption studies

After the column is completely exhausted, the remaining aqueous solution in the column is drained off by pumping air through the column. Desorption of solute from loaded adsorbent is carried out by 0.1 M NaOH solution as an eluent. The eluent is pumped in to the column at a fixed flow rate of  $1 \text{ ml min}^{-1}$  at constant temperature. From the start of the desorption process, effluent samples are collected at different time intervals and the concentration of the adsorbates are determined. When the concentration of the outlet solution is zero or close to zero, it is assumed that the column is regenerated. After the regeneration, the adsorbent column is washed with distilled water to remove NaOH from the column before the influent adsorbate solution (phenol or *o*-chlorophenol) is reintroduced for the subsequent adsorption–desorption cycles. The adsorption–desorption cycles are performed thrice for each phenolic solution using the same bed to check the sustainability of the bed for repeated use. Regeneration curves are obtained by plotting volume of the solution passed through the column vs. concentration of the column outlet solution.

### 3. Results and discussion

#### 3.1. Characterization of CS/Ca alginate beads

##### 3.1.1. Surface analysis

Surface area, density, pore volume, pore diameter and porosity of the composite biosorbent are determined with BET and Pycnomatic ATC instruments. The isotherm plots are used to calculate the specific surface area ( $N_2$ /BET method) and average pore diameter of CS/Ca beads, while micropore volume is calculated from the volume of nitrogen adsorbed at  $p/p_0$  1.3. The sorbent material shows an average surface area of  $102.15 \text{ m}^2 \text{ g}^{-1}$ , pore volume of  $0.5 \text{ cm}^3 \text{ g}^{-1}$ , porosity of 52.36%, pore diameter of 0.87 nm and density of  $2.15 \text{ g cm}^{-3}$ .

##### 3.1.2. Fourier transform infrared spectral analysis

The FTIR spectrum of CS/Ca alginate beads synthesized from sodium alginate and chitosan and blended with  $\text{CaCl}_2$  is shown in Fig. 1a. The broad band in the region between  $3000$  and  $3700 \text{ cm}^{-1}$  is due to overlapping of the stretching frequencies of  $-\text{OH}$  and  $-\text{NH}_2$  groups. The bands at  $2922.0$  and  $1428.1 \text{ cm}^{-1}$  represent stretching and bending frequencies of  $-\text{CH}_2$  group. The bands at  $1645.7$  and  $1076.9 \text{ cm}^{-1}$  are observed due to the bending and stretching of  $-\text{NH}_2$  and  $-\text{COO}^-$  groups, respectively. The presence of  $-\text{C}-\text{O}$  and  $-\text{C}-\text{N}$  linkages are confirmed from the peaks at  $1316.4$  and  $1021.5 \text{ cm}^{-1}$ . The FTIR spectra of the biosorbent loaded with phenol and *o*-chlorophenol are given in Fig. 1b and c, respectively. In the spectra a new band is observed at  $1582 \text{ cm}^{-1}$ , which can be assigned to a symmetric  $-\text{NH}_2$  deformation. Further, the figures indicate that there is a shift in absorption frequency of amino and hydroxyl groups, which signify the deformation of  $-\text{OH}$ ,  $-\text{COO}^-$ , and  $-\text{NH}$  bonds. These may be attributed to the interaction between the functional groups of alginate and chitosan with phenolic compounds during the adsorption process. These results confirm the

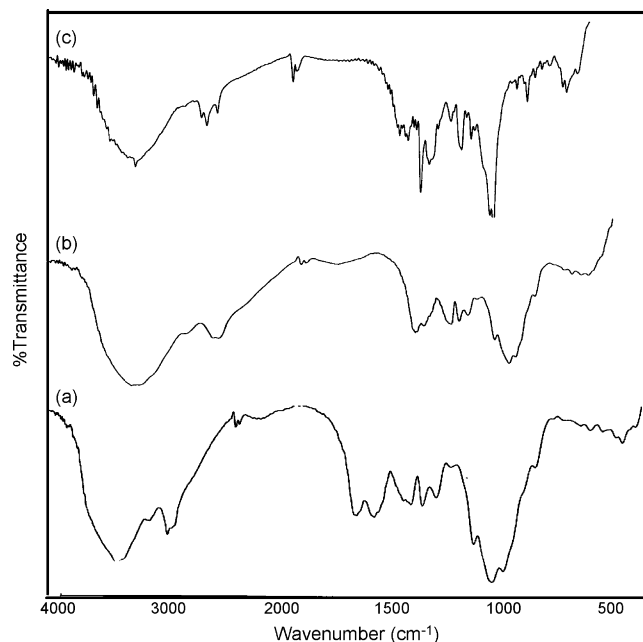


Fig. 1. FTIR spectrum of CS/Ca alginate blended beads (a), after adsorption of phenol (b) and after adsorption of *o*-chlorophenol (c).

participation of amino, carboxylic and hydroxyl groups of CS/Ca blended beads as potential active binding sites for adsorption of phenolic compounds.

##### 3.1.3. XRD analysis

A Siemens D 5000 powder X-ray diffractometer is used to study the solid-state morphology of CA/Ca alginate blended beads. X-rays of  $1.5406 \text{ \AA}$  wavelength are generated by a  $\text{Cu K}\alpha$  source. The angle of diffraction is varied from  $10$  to  $60^\circ$  to identify the change in the crystal structure and intermolecular distances between inter segmental chains after adsorption process of phenolic compounds on CS/Ca alginate blended beads.

Wide-angle X-ray diffractogram of the beads, shown in Fig. 2a, indicates the amorphous nature of the sorbent as there is no peak observed. Smitha et al. [28] reported that the membrane synthesized from sodium alginate and chitosan is amorphous compared to both alginate and chitosan. Fig. 2b and c shows diffractograms of sorbent after adsorption of phenol and *o*-chlorophenol on CS/Ca alginate beads, in which the peaks are appearing at  $30.3$  and  $30.6^\circ$

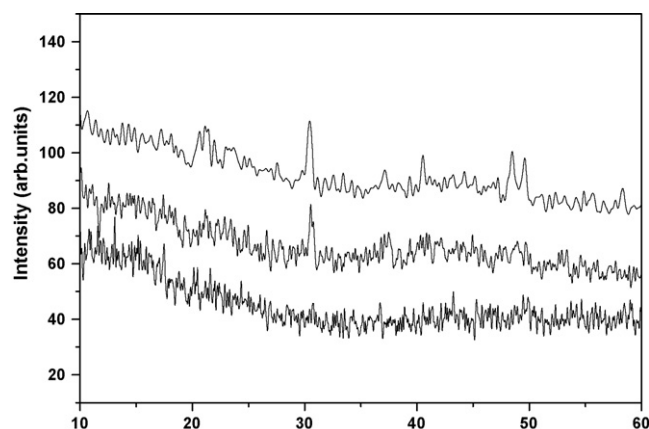


Fig. 2. Wide-angle X-ray diffraction patterns of CS/Ca alginate beads: (a) before adsorption, (b) after adsorption of phenol and (c) after adsorption of *o*-chlorophenol.

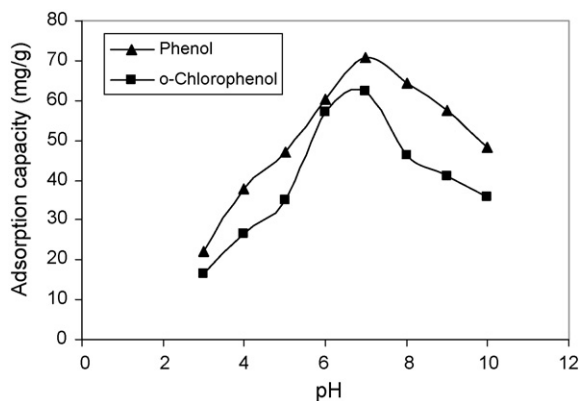


Fig. 3. Effect of pH on adsorption of phenol and *o*-chlorophenol on CS/Ca alginate beads.

of  $2\theta$  value for phenol and *o*-chlorophenol, respectively. From these figures, it is observed that after adsorption of phenolic compounds, CS/Ca alginate beads appear as of semi-crystalline in nature. The existence of semi-crystalline structure in the beads after adsorption may be attributed to the possibility of nucleation process or complex formation between the functional groups present in the beads with phenolic compounds and also may be partially due to hydration.

### 3.2. Effect of pH

The effect of solution pH on the removal of phenol and their derivatives from aqueous solution could be explained by considering the presence of ionic and molecular forms of phenolic compounds in aqueous solution. These compounds act as weak acids in aqueous solution, and the dissociation of hydrogen ion from phenolic compounds strongly depends on the pH of the solution. In acidic solutions, the molecular form dominates and in alkaline medium, the anionic form is the predominant species. In order to optimize the pH for maximum removal efficiency, experiments are conducted in the pH range from 3.0 to 10.0 using 0.1 g of CS/Ca alginate beads with 100 ml of 100 ppm adsorbate solutions at room temperature. These results are graphically represented in Fig. 3. The results indicate that the extent of adsorption varies with pH. Under acidic conditions (below pH 3) the beads undergo dissolution. Due to this, experiments are conducted above pH 3.0. Experimental results show that the phenol and *o*-chlorophenol are removed more effectively by CS/Ca alginate beads at around pH 7.0 and decreased on either sides of pH 7.0. Both phenol and *o*-chlorophenol exist predominantly as neutral species at pH 7.0. The interaction between the CS/Ca alginate beads and phenolic derivatives is considered mainly as non-polar, and the forces responsible for adsorption are physical van der Waals forces. This behavior provides potential for recovery of the adsorbate as well as regeneration of adsorbent by simple non-destructive methods such as solvent washing. Comparing phenol and *o*-chlorophenol, the sorbent shows more adsorption capacity towards the former than the latter. This aqueous solubility of phenol (8.0 g/100 g of water) is more compared to *o*-chlorophenol (2.85 g/100 g of water). Compared to phenol, *o*-chlorophenol would have shown more affinity towards non-aqueous medium as evidenced by their octanol–water partition coefficients ( $\log k_{ow}$  of phenol is 1.46 and of *o*-chlorophenol is 2.15). Based on aqueous solubility and octanol–water partition coefficient, *o*-chlorophenol is expected to adsorb to a greater extent compared to phenol. But experimental results indicate that the extent of adsorption of phenol is more than that of *o*-chlorophenol. The adsorption of phenol

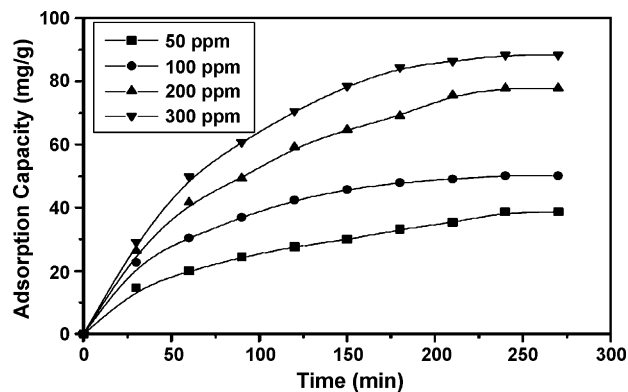


Fig. 4. Effect of agitation time on adsorption of phenol on CS/Ca alginate beads at different initial concentrations.

and *o*-chlorophenol cannot be correlated to physical parameters such as solubility and octanol–water partition coefficients. Calace et al. [29] observed similar trend in adsorption of phenols on paper mill sludge. The sorbent developed in the present study exhibits an maximum monolayer adsorption capacity of  $108.7 \text{ mg g}^{-1}$  for phenol and  $97.1 \text{ mg g}^{-1}$  for *o*-chlorophenol as obtained from Langmuir adsorption isotherm. These values are higher compared with those reported in the literature. The maximum adsorption capacity as reported in the literature for phenol is  $28.14 \text{ mg g}^{-1}$  on calcium alginate [21] and  $63.69 \text{ mg g}^{-1}$  on chitosan coated bentonite [24]. Juan et al. [20] reported the adsorption capacity of calcium alginate as  $1.63 \text{ mg g}^{-1}$  for 2,4-dichlorophenol.

### 3.3. Sorption kinetics

#### 3.3.1. First-order kinetics

Data on removal of phenol and *o*-chlorophenol by CS/Ca alginate beads as a function of time at pH 7.0 at various initial concentrations (50–300 ppm) are presented graphically in Figs. 4 and 5. From the figures it is observed that the adsorption capacity of phenol and *o*-chlorophenol increases to saturation with time and maximum adsorption is attained at 240 min. Therefore, these times are sufficient to attain equilibrium for the maximum removal of phenol and *o*-chlorophenol from aqueous solution on CS/Ca alginate beads. The first-order kinetic parameters of adsorption of these adsorbates on CS/Ca alginate beads are determined using Lagergren's equation

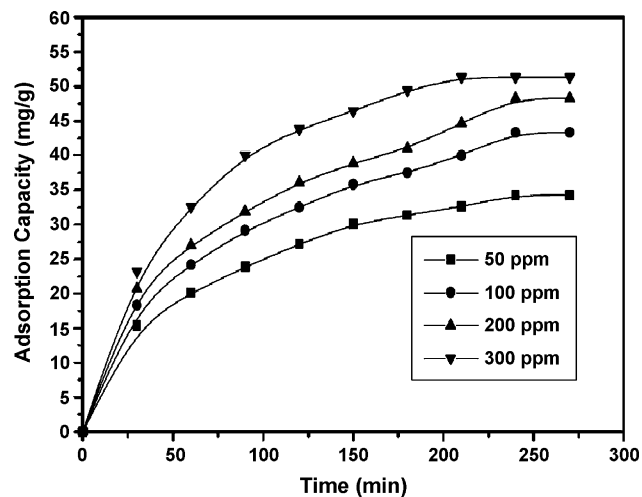


Fig. 5. Effect of agitation time on adsorption of *o*-chlorophenol on CS/Ca alginate beads at different initial concentrations.

**Table 1**  
Adsorption rate constants of Lagergren first-order kinetics for phenol and *o*-chlorophenol on CS/Ca alginate beads

Initial concentrations of adsorbents (ppm)	Phenol		<i>o</i> -Chlorophenol	
	$K_{ad}$	$r^2$	$K_{ad}$	$r^2$
50	0.0101	0.998	0.0124	0.992
100	0.0111	0.995	0.0108	0.987
200	0.0111	0.996	0.0105	0.966
300	0.0119	0.994	0.0113	0.985

[30]:

$$\log(Q_e - Q_t) = \log Q_e - \left(\frac{K_{ad}}{2.303}\right) t \quad (2)$$

where  $Q_e$  is the amount of sorbate adsorbed per unit weight of sorbent at equilibrium ( $\text{mg g}^{-1}$ ),  $Q_t$  is the amount of sorbate uptake per unit weight of sorbent at any time  $t$  ( $\text{mg g}^{-1}$ ),  $t$  is the time in minutes and  $K_{ad}$  ( $\text{min}^{-1}$ ) is the rate constant of adsorption. The values of  $K_{ad}$ , calculated from the slopes of the plot of  $\log(Q_e - Q_t)$  vs.  $t$ , are given in Table 1 along with the correlation coefficients ( $r^2$ ). There is no significant change in the values of  $K_{ad}$  at various concentrations of phenol and *o*-chlorophenol. From this observation it may be concluded that the adsorption of phenolic compounds on the CS/Ca alginate beads follow first-order kinetics.

3.3.2. Second-order kinetics

Experimental data are also fitted to the pseudo-second-order kinetic model, which is given in the following form [31]:

$$\frac{t}{Q_t} = \frac{1}{K_2 Q_e^2} + \frac{1}{Q_e} t \quad (3)$$

where  $K_2$  ( $\text{g mg}^{-1} \text{min}^{-1}$ ) is the rate constant of the second-order equation,  $Q_t$  ( $\text{mg g}^{-1}$ ) is the amount adsorbed at time  $t$  (min) and  $Q_e$  is the amount adsorbed at equilibrium ( $\text{mg g}^{-1}$ ). This model is more likely to predict the kinetic behavior of adsorption with chemical sorption being the rate-controlling step [32,33]. The rate constants ( $k_2$ ), calculated from the slopes of the plots of  $t/Q_t$  vs.  $t$  along with correlation coefficients and  $Q_e$  values, are given in Table 2. From Tables 1 and 2 it is observed that the experimental data are well fitted to Lagergren first-order kinetic model compared to second-order kinetics model.

3.3.3. Weber–Morris method

An intraparticle diffusion model proposed by Weber and Morris [34] can be written as follows:

$$Q_t = k_{id} t^{1/2} + C \quad (4)$$

where  $Q_t$  ( $\text{mg l}^{-1}$ ) is the amount adsorbed at time  $t$  (min), and  $k_{id}$  ( $\text{mg g}^{-1} \text{min}^{-1/2}$ ) is the rate constant of intraparticle diffusion.  $C$  is the value of the intercept, which gives an idea about the boundary layer thickness, i.e., the larger the intercept; the greater is the boundary layer effect.

The plots of  $Q_t$  vs.  $t^{1/2}$  obtained for the adsorption of phenol and *o*-chlorophenol onto CS/Ca alginate beads at different concentra-

**Table 2**  
Constants of second-order kinetic equation for adsorption of phenol and *o*-chlorophenol on CS/Ca alginate beads

Concentration (ppm)	Phenol			<i>o</i> -Chlorophenol		
	$Q_e$ (mg/g)	$K_2 (\times 10^4)$	$r^2$	$Q_e$ (mg/g)	$K_2 (\times 10^4)$	$r^2$
50	51.0	1.960	0.9987	41.5	4.029	0.9932
100	71.4	1.854	0.9956	50.8	3.174	0.9929
200	95.2	1.462	0.9955	55.6	2.968	0.9891
300	116.3	1.158	0.9915	64.9	2.718	0.9989

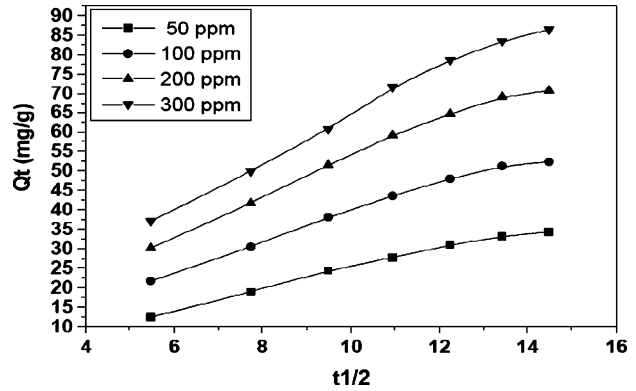


Fig. 6. Weber–Morris model plot for adsorption of phenol on CS/Ca alginate beads.

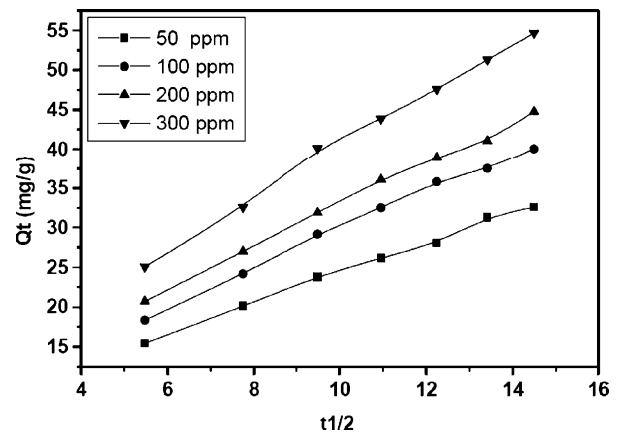


Fig. 7. Weber–Morris model plot for adsorption of *o*-chlorophenol on CS/Ca alginate beads.

tions are shown in Figs. 6 and 7, respectively. The intraparticle rate constant  $k_{id}$  ( $\text{mg g}^{-1} \text{min}^{-1/2}$ ) and intercept  $C$  ( $\text{mg g}^{-1}$ ) are given in Table 3. The values of correlation coefficients ( $r^2$ ) for the intraparticle diffusion model are lower than that of the pseudo-second-order kinetic model. Moreover, intraparticle diffusion cannot be accepted as a rate-controlling step for the adsorption of both adsorbates onto CS/Ca alginate beads due to the fact that values of  $C$  are not constant and vary with the concentration of the adsorbate (Table 3).

3.4. Effect of adsorbent dose

The results of the experiments with varying amount of adsorbent are represented in Fig. 8 with increase in adsorbent dose, from 0.05 to 0.4 g, while keeping the volume and concentration of the solution constant. From the figure, it is apparent that the percent removal of phenol and *o*-chlorophenol increases rapidly with increase in the dose of CS/Ca alginate beads due to the greater availability of binding sites of the biosorbent. Adsorption is maximum with 0.4 g of CS/Ca alginate beads and the maximum

**Table 3**  
Parameters of Web–Morris equation for adsorption of phenol and *o*-chlorophenol on CS/Ca alginate beads

Concentration (ppm)	Phenol			<i>o</i> -Chlorophenol		
	$k_{id}$	$C$	$r^2$	$k_{id}$	$C$	$r^2$
50	2.2978	2.1821	0.9982	1.9097	5.2148	0.9955
100	3.5406	3.4267	0.985	2.4099	5.6572	0.9946
200	4.6732	5.9953	0.986	2.6156	6.7437	0.9965
300	5.7113	6.5578	0.9901	3.27	7.6628	0.9959

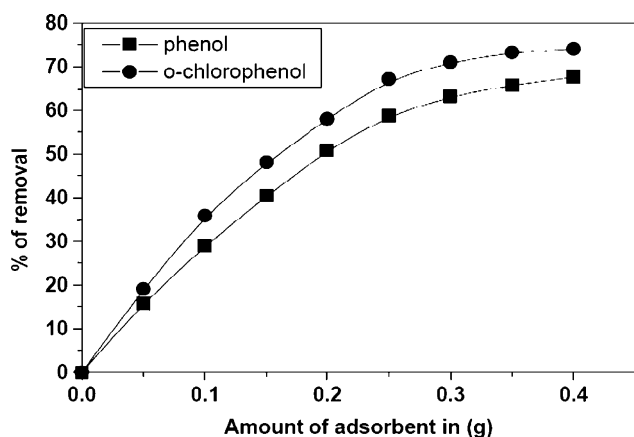


Fig. 8. Effect of dose of adsorbent (CS/Ca alginate beads) on percent removal of phenol and *o*-chlorophenol.

percent removal is about 68% with phenol and about 74% with *o*-chlorophenol.

### 3.5. Adsorption isotherm models

An adsorption isotherm describes the relationship between the amount of adsorbate that is adsorbed on the adsorbent and the concentration of dissolved adsorbate in the liquid at equilibrium. Several models have been published in the literature to describe experimental data of adsorption isotherms. Three important isotherms are selected in this study, namely, the Langmuir, Freundlich and Dubinin–Radushkevich (D–R) isotherm models. The Langmuir and Freundlich models are the most frequently used models. The Langmuir model is obtained under the ideal assumption of a totally homogenous adsorption surface, whereas the Freundlich isotherm is suitable for a highly heterogeneous surface. The Dubinin–Radushkevich isotherm, on the other hand, is based on the potential theory of adsorption for adsorbents with an energetically non-uniform surface where the dominant adsorption interaction is dispersion forces.

The Langmuir theory was first used to describe the adsorption of gas molecules on to solvent solution surfaces [35]. However, this model has found successful application in many other sorption processes. The Langmuir model can be expressed by:

$$Q_e = \frac{Q^0 b C_e}{1 + b C_e} \quad (5)$$

where  $Q_e$  is the amount of solvents adsorbed ( $\text{mg g}^{-1}$ ),  $C_e$  is the equilibrium concentration of adsorbate ( $\text{mg l}^{-1}$ );  $Q^0$  and  $b$  are Langmuir constants related to adsorption capacity and energy of adsorption, respectively.

The empirical model proposed by Freundlich is shown to be consistent with an exponential distribution of active centers, characteristic of heterogeneous surfaces. The amount of sorbate adsorbed,  $Q_e$ , is related to the concentration of sorbate in the solu-

tion,  $C_e$ , through the following equation:

$$Q_e = K_f C_e^{1/n} \quad (6)$$

where  $K_f$  and  $n$  are Freundlich constants. Experimental data of the present study are fitted to Eq. (6) and the parameters ( $K_f$  and  $n$ ) are evaluated from the plot of  $\log Q_e$  vs.  $\log C_e$ . The values of Langmuir constants  $Q^0$  and  $b$  and Freundlich parameters  $K_f$  and  $n$  along with the correlation coefficients ( $r^2$ ) are presented in Table 4. Among, these two models, the experimental data are well fitted to Langmuir compared to Freundlich model.

The equilibrium data are also correlated with the Dubinin–Radushkevich (D–R) model to determine if adsorption occurred by physical or chemical processes [36]. Mathematically the model is represented as:

$$Q = Q_e e^{-k\varepsilon^2} \quad (7)$$

Linearized form of the equation is given as:

$$\ln Q = \ln Q_e - k\varepsilon^2 \quad (8)$$

where  $\varepsilon$  is the Polanyi potential,  $Q$  is the amount of solute adsorbed per unit weight of adsorbent ( $\text{mol g}^{-1}$ ),  $k$  is a constant related to the adsorption energy ( $\text{mol}^2 \text{kJ}$ ) and  $Q_m$  is the adsorption capacity ( $\text{mol g}^{-1}$ ).

The values of  $Q_m$  and  $k$  were calculated from the intercept and slope of the  $\ln Q$  vs.  $\varepsilon^2$  plots and presented in Table 4. The mean free energy of adsorption ( $E$ ), defined as the free energy change when one mole of ions is transferred to the surface of the solid from infinity in solution can be calculated from  $k$  value using the equation:

$$E = (-2k)^{-0.5} \quad (9)$$

The magnitude of  $E$  is useful for estimating the type of adsorption process. The mean free energy of adsorption  $E$ , gives information about adsorption mechanism as chemical ion-exchange or physical adsorption. The magnitude of  $E$  is between 8 and 16 kJ/mol, the adsorption process follows chemical ion-exchange while for the values of  $E < 8$  kJ/mol, the adsorption process is of a physical nature [37]. The mean adsorption energy ( $E$ ) was calculated as 12.5 kJ/mol for phenol and 15.81 kJ/mol for *o*-chlorophenol on to CS/Ca alginate beads. These values indicate that the adsorption processes is associated with chemical ion-exchange mechanism. Actually, chitosan can interact with adsorbates through physical as well as chemical forces to varying degrees depending on the conditions.

### 3.6. Column adsorption data

The results of dynamic flow experiments are used to obtain the breakthrough curves for adsorption of phenol and *o*-chlorophenol from aqueous solutions by plotting bed volume vs. effluent concentration. The breakthrough curves are shown in Figs. 9 and 10. The breakthrough capacity, which is the amount adsorbed until the effluent concentration of the adsorbate is equal to the influent solution concentration, are computed from the breakthrough curves. An examination of the curves indicates that no leakage of solute is observed up to a volume of about 100 ml of the influent solution in the first cycle.

Table 4

Parameters of Langmuir, Freundlich and D–R isotherms for adsorption of phenol and *o*-chlorophenol on CS/Ca alginate beads

Adsorbate	Langmuir constants			Freundlich constants			Dubinin–Radushkevich isotherm			
	$Q^0$	$b$	$r^2$	$K_f$	$n$	$r^2$	$K$	$\ln Q^0$	$E$	$r^2$
Phenol	108.69	0.0120	0.9883	1.966	1.2918	0.9383	0.0032	3.584	12.5	0.9912
<i>o</i> -Chlorophenol	97.08	0.0166	0.9802	2.977	1.4920	0.9106	0.0020	3.587	15.8	0.9983

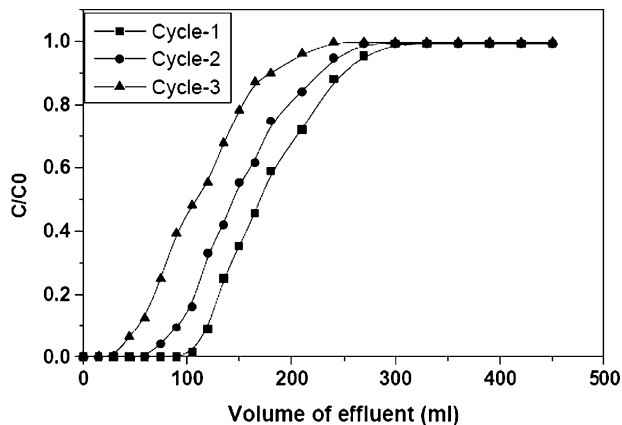


Fig. 9. Column break through curves for adsorption of phenol on CS/Ca alginate beads.

When the bed is exhausted or the effluent coming out of the column reaches the allowable maximum discharge level, the regeneration of the adsorption bed to recover the adsorbed material and/or to regenerate the adsorbent becomes quite essential. The regeneration could be accomplished by a variety of techniques such as thermal desorption, steam washing, solvent extraction, etc. Each method has inherent advantages and limitations. In this study, several solvents are tried to regenerate the adsorption bed. 0.1 M NaOH solution is found to be effective in desorbing and recovering adsorbates quantitatively from the adsorption bed. The fixed bed columns of CS/Ca alginate beads saturated with phenol or chlorophenol is regenerated by passing 0.1 M NaOH solution as an eluent at a fixed flow rate of  $1 \text{ ml min}^{-1}$ . To evaluate the solvent recovery efficiency, the percent of phenol and *o*-chlorophenol recovered is calculated from the breakthrough and recovery curves. The desorption profile is graphically represented in Figs. 11 and 12. From the plots it is observed that the rate of desorption increases sharply reaching a maximum with 8 and 6 ml of 0.1 M NaOH solution. The regenerated column is further used for the removal of phenol. The results indicate that the column gets saturated early and adsorption capacity decreases. As a result, the percent desorption also decreases from first cycle to second cycle. Similar behavior is observed in case of third cycle of adsorption–desorption experiments.

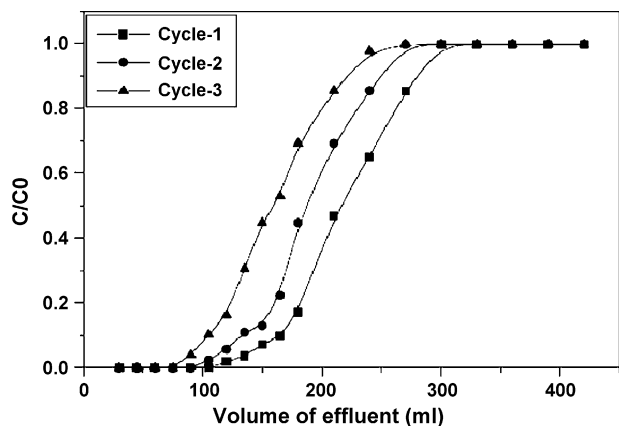


Fig. 10. Column break through curves for adsorption of *o*-chlorophenol on CS/Ca alginate beads.

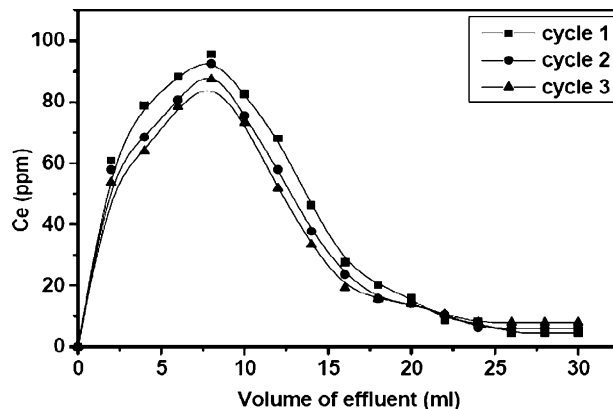


Fig. 11. Regeneration curves of CS/Ca alginate beads loaded with phenol.

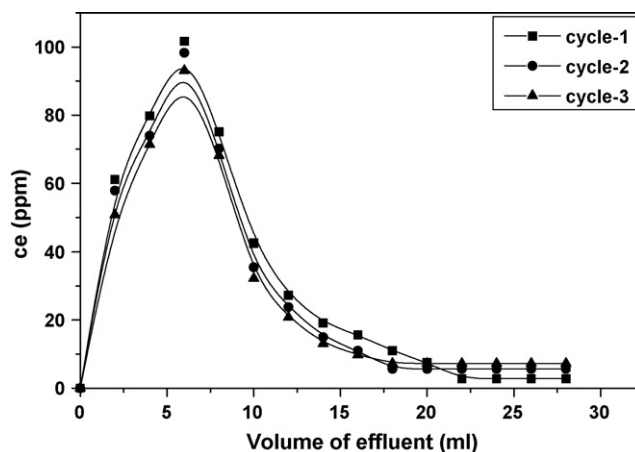


Fig. 12. Regeneration curves of CS/Ca alginate beads loaded with *o*-chlorophenol.

#### 4. Conclusions

It is demonstrated in this study that removal of phenol and *o*-chlorophenol from aqueous solutions is feasible through adsorption on CS/Ca alginate beads at neutral pH under equilibrium and column flow experimental conditions. The adsorption capacity is maximum around pH 7.0 and decreases significantly on either side of pH 7.0. Langmuir and D–R isotherm models represent the experimental data adequately and better than Freundlich isotherm model. Experimental kinetic data are also fitted to first-order, second-order and Web–Morris kinetic equations and the rate constants are evaluated. The results indicate that CS/Ca alginate beads show higher adsorption capacity for phenol than *o*-chlorophenol. Further, results from the limited number of column adsorption–desorption cycle indicates that the adsorption capacity of the CS/Ca alginate beads decreases in the second and third adsorption–desorption cycles.

#### References

- [1] J. Wu, H.Q. Yu, Biosorption of phenol and chlorophenols from aqueous solutions by fungal mycelia, *Process Biochem.* 41 (2006) 44–49.
- [2] E. Rubin, P. Rodriguez, Adsorption of phenolic compounds by the brown alga *Sargassum muticum*, *J. Chem. Technol. Biotechnol.* 81 (2006) 1093–1099.
- [3] A. Dabrowski, P. Podkoscielny, Z. Hubicki, M. Barczak, Adsorption of phenolic compounds by activated carbon—a critical review, *Chemosphere* 58 (2005) 1049–1070.
- [4] A. Krishnaiah, Adsorption of phenol and *p*-chlorophenol from their single and bisolute aqueous solutions on Amberlite XAD–16 resin, *J. Hazard. Mater.* B105 (2003) 143–156.

- [5] I. Efremenko, M. Sheintuch, Predicting solute adsorption on activated carbon: phenol, *Langmuir* 22 (2006) 3614–3621.
- [6] F.A. Banat, B.Al. Bashir, S.Al. Asheh, O. Hayajneh, Adsorption of phenol by bentonite, *Environ. Pollut.* 107 (2000) 391–398.
- [7] S. Rengaraj, S. Moon, R. Sivabalan, B. Arabindoo, V. Murugesan, Removal of phenol from aqueous solution and resin manufacturing industry wastewater using an agricultural waste: rubber seed coat, *J. Hazard. Mater.* B89 (2002) 185–196.
- [8] E. Tütem, R. Apak, Ç.F. Ünal, Adsorptive removal of chlorophenols from water by bituminous shale, *Water Res.* 32 (1998) 2315–2324.
- [9] K.S. Kader Abdul, J. Uthayavani, E. Subramanian, Adsorption characteristics of chlorophenols from aquatic systems by hypercrosslinked resins modified with benzoyl group, *Indian J. Environ. Prot.* 18 (1998) 181.
- [10] E. Mona, R. Zein, R. Kurniadi, I. Kurniadi, The use of rice husk for removal of phenol from waste water as studied using 4-aminoantipyrine spectrophotometric method, *Environ. Technol.* 18 (1997) 355–358.
- [11] M.S. Baggily, Adsorption of 4-chlorophenol from aqueous solutions by XAD-4 resin: isotherm kinetic thermodynamic analysis, *J. Hazard. Mater.* B137 (2006) 157–164.
- [12] C. Wu-Chung, F. Tzu-Ping, Mechanism of removing chlorophenolic compounds from solution by a water-insoluble cationic starch, *J. Polym. Res.* 4 (1997) 47–55.
- [13] A. Batnagar, Removal of bromophenols from water using industrial wastes as low cost adsorbents, *J. Hazard. Mater.* B139 (2007) 93–102.
- [14] A. Kuleyin, Removal of phenol and *p*-chlorophenol by surfactant modified natural zeolite, *J. Hazard. Mater.* B144 (2007) 307–315.
- [15] D. Tang, Z. Zheng, K. Lin, J. Luan, J. Zhang, Adsorption of *p*-nitrophenol from aqueous solutions onto activated carbon fiber, *J. Hazard. Mater.* B143 (2007) 49–56.
- [16] J.S. Rhee, M.W. Jung, K.J. Paeng, Evaluation of chitin and chitosan as a sorbent for the preconcentration of phenol and chlorophenols in water, *Anal. Sci.* 14 (1998) 1089–1092.
- [17] K. Inoue, K. Yoahizuka, Y. Baba, Adsorption of metal ions on chitosan and its derivatives, in: M. Abe, T. Suzuki (Eds.), *New Development in Ion Exchange*, Kodansha, Tokyo, 1996.
- [18] R.S. Juang, C.Y. Ju, Kinetics of sorption of Cu(II)-ethylenediaminetetraacetic acid chelated anions on cross-linked polyaminated chitosan beads, *Ind. Eng. Chem. Res.* 32 (1998) 386.
- [19] J. Trivedi Umang, S. Bassi Amarjeet, Z. Jingxu, Investigation of phenol removal using sol-gel/alginate immobilized soybean seed hull peroxidase, *Can. J. Chem. Eng.* 84 (2006) 239–247.
- [20] W. Juan, Y. Han-Qing, Biosorption of 2,4-dichlorophenol by immobilized white-rot fungus *Phanerochaete chrysosporium* from aqueous solutions, *Bioresour. Technol.* 98 (2007) 253–259.
- [21] Y. Jodra, F. Mijangos, Phenol adsorption in immobilized activated carbon with alginate gels, *Sep. Sci. Technol.* 38 (2003) 1851–1867.
- [22] K. Yamada, Y. Akiba, T. Shibuya, A. Kashiwada, K. Matsuda, M. Hirata, Water purification through bioconversion of phenol compounds by tyrosinase and chemical adsorption by chitosan beads, *Biotechnol. Prog.* 21 (2005) 823–829.
- [23] N. Aoki, K. Kinoshita, K. Mikuni, K. Nakanishi, K. Hattori, Adsorption of 4-nonylphenol ethoxylates onto insoluble chitosan beads bearing cyclodextrin moieties, *J. Incl. Phenom. Macrocycl. Chem.* 57 (2007) 237–241.
- [24] T. Cheng, S. Wang, Q. Xu, J. Yan, Study on the adsorption capacity of phenol by chitosan coated bentonite, *Chemical* 20 (2006) 1–3.
- [25] A. Badwan, A. Abumaloo, A. Sallam, A. Abukalaf, O. Jawan, A sustained release drug delivery system using calcium alginate beads, *Drug. Dev. Ind. Pharm.* 11 (1985) 239–248.
- [26] S.J. Rendevski, A.N. Andonovski, Reaggregation of sodium alginate microgel structures after shear-induced deaggregation at filtering, *Polym. Bull.* 54 (2005) 93–100.
- [27] S. Roger, D. Talbot, A. Bee, Preparation and effect of Ca<sup>2+</sup> ions on water solubility, particle release and swelling properties of magnetic alginate films, *J. Magn. Mater.* 305 (2006) 221–227.
- [28] B. Smitha, S. Sridhar, A.A. Khan, Chitosan–sodium alginate polyion complexes as fuel cell membranes, *Eur. Polym. J.* 41 (2005) 1859–1866.
- [29] N. Calace, E. Nardi, B.M. Petronio, M. Pietroletti, Adsorption of phenols by paper mill sludge, *Environ. Pollut.* 118 (2002) 315–319.
- [30] S. Lagergren, Zur theorie der sogenannten adsorption geloster stoffe, *Kungliga Svenska Vetenskapsakademiens, Handlingar* 24 (1998) 1–39.
- [31] Y.S. Ho, G. McKay, Pseudo-second order model for sorption processes, *Prog. Biochem.* 34 (1999) 451–465.
- [32] Y.S. Ho, G. McKay, Kinetic models for the sorption of dye from aqueous solution by wood, *J. Environ. Sci. Health B: Process Saf. Environ. Prot.* 76 (1998) 183–191.
- [33] K.G. Bhattacharyya, A. Sharma, Azadirachta indica leaf powder as an effective biosorbent for dyes; a case study with aqueous Congo Red solutions, *J. Environ. Manage.* 71 (3) (2004) 217–229.
- [34] W.J. Weber Jr., J.C. Morriss, Kinetics of adsorption on carbon from solution, *J. Sanit. Eng. Div. Am. Soc. Civ. Eng.* 89 (1963) 31–60.
- [35] B. Benguella, H. Benaissa, Cadmium removal from aqueous solutions by chitin, Kinetic and equilibrium studies, *Water Res.* 36 (2002) 2463–2474.
- [36] N. Unlu, M. Ersoz, Adsorption characteristics of heavy metal ions onto a low cost biopolymeric sorbent from aqueous solutions, *J. Hazard. Mater.* B136 (2006) 272–280.
- [37] A. Kilislioglu, B. Bilgin, Thermodynamic and kinetic investigation of uranium adsorption on amberlite IR-118H resin, *Appl. Radiat. Isot.* 58 (2003) 155–160.